

# Classical analogies for the force acting on an impurity in a Bose-Einstein condensate

Jonas Rønning<sup>1</sup>, Audun Skaugen<sup>2</sup>, Emilio Hernández-García<sup>3</sup>,  
Cristóbal López<sup>3</sup>, Luiza Angheluta<sup>1</sup>

<sup>1</sup>PoreLab, The Njord Centre, Department of Physics, University of Oslo, P. O. Box 1048, 0316 Oslo, Norway

<sup>2</sup>Computational Physics Laboratory, Tampere University, P.O. Box 692, FI-33014 Tampere, Finland

<sup>3</sup>IFISC (CSIC-UIB), Instituto de Física Interdisciplinar y Sistemas Complejos, 07122 Palma de Mallorca, Spain

## Abstract.

We study the hydrodynamic forces acting on a small impurity moving in a two-dimensional Bose-Einstein condensate at non-zero temperature. The condensate is modelled by the damped-Gross Pitaevskii (dGPE) equation and the impurity by a Gaussian repulsive potential coupled to the condensate. For weak coupling, we obtain analytical expressions for the forces acting on the impurity, and compare them with those computed through direct numerical simulations of the dGPE and with the corresponding expressions for classical forces. For non-steady flows, there is a time-dependent force dominated by inertial effects and which has a correspondence in the Maxey-Riley theory for particles in classical fluids. In the steady-state regime, the force is dominated by a self-induced drag. Unlike at zero temperature, where the drag force vanishes below a critical velocity, at low temperatures the impurity experiences a net drag even at small velocities, as a consequence of the energy dissipation through interactions of the condensate with the thermal cloud. This dissipative force due to thermal drag is similar to the classical Stokes' drag. There is still a critical velocity above which steady-state drag is dominated by acoustic excitations and behaves non-monotonically with impurity's speed.

## **1. Introduction**

The motion of an impurity suspended in a quantum fluid depends on several key factors such as the superfluid nature and flow regime, as well as the size of the impurity and its interaction with the surrounding fluid [1, 2, 3, 4, 5]. Therefore, it is disputable whether the forces acting on an impurity in a quantum fluid should bear any resemblance to classical hydrodynamic forces. In the case of an impurity immersed in superfluid liquid helium, classical equations of motion and hydrodynamic forces are assumed a priori [6], since impurities are typically much larger than the coherence length and then quantum hydrodynamic effects like the quantum pressure can be neglected. For Bose-Einstein condensates (BEC) in dilute atomic gases, impurities can be neutral atoms [7], ion impurities [8, 9] or quasiparticles [10]. The size of an impurity in a BEC is typically of the same order of magnitude or smaller than the coherence length, and quantum hydrodynamic effects cannot be readily ignored.

There are several theoretical and computational studies of the interaction force between an impurity and a BEC at zero absolute temperature, using different approaches depending on the nature of the particle and its interaction with the condensate. A microscopic approach is used to analyse the interaction of a rigid particle with a BEC by solving the Gross-Pitaevskii equation (GPE) for the condensate macroscopic wavefunction and using boundary conditions such that the condensate density vanishes at the particle boundary [11]. This methodology allows to study complex phenomena such as vortex nucleation and flow instabilities, but it is more oriented to find the effects of an obstacle on the flow rather than the coupled particle-flow dynamics. In addition, the boundary condition introduces severe nonlinearities which can only be addressed numerically. At a more fundamental level of description, the impurity is treated as a quantum particle with its own wavefunction described by the Schrödinger equation and that is coupled with the GPE for the macroscopic wavefunction of the BEC [12]. A more versatile model for the interaction of impurities with the BEC has been explored in several papers [3, 4, 13, 14, 5, 15]. Here, an additional repulsive interaction (a Gaussian or delta-function potential) is added to model scattering of the condensate particles with the impurity. The force on the impurity is determined by this repulsion potential and the superfluid density through the Ehrenfest theorem. The strong-coupling limit of this repulsive potential would be equivalent to the rigid boundary-condition approach. Within this modelling approach, some works have studied the complex motion of particles interacting with vortices in the flow, and the indirect interactions between them arising from the presence of the fluid [4, 14]. Another line of research using this type of modelling focused mainly on the superfluidity criterion of an equilibrium BEC [3, 16, 17, 18, 19, 5] and non-equilibrium BEC at zero temperature [20]. Within the Bogoliubov perturbation analysis for a small impurity with weak coupling, analytical expressions can be derived for the steady-state force on the impurity. At zero temperature, this force vanishes below a critical velocity and corresponds to the dissipationless motion. Above this velocity identified through Landau criterion as the

speed of the long-wavelength sound waves, there is a net drag force and the motion of the impurity is damped by acoustic excitations. While this is a form of drag, in that the force opposes motion by dissipating energy, it is not the same as the classical Stokes' drag in viscous fluids. Recent experiments probing superfluidity in a BEC are able to indirectly estimate the drag force by measuring the local heating rate in the vicinity of the moving laser beam and show that there is still a critical velocity even at non-zero temperatures and that the critical velocity is lower for a repulsive potential than for an attractive one [21].

In this paper, we study the forces exerted on an impurity moving in a two-dimensional BEC at low temperature, using an approach similar to [3, 4, 13, 14, 5], in which a repulsive Gaussian potential is used to describe the interaction of the particle with the BEC, but using a dissipative version of the GPE. Our aim is to bridge this microscopic approach with the phenomenological descriptions [6] that assume that the forces from the superfluid are the same as those from a classical fluid in the inviscid and irrotational case. As in the classical-fluid case, we find that the force is made of two contributions: One of them, dominant for very weak fluid-particle interaction, bears a rather complete analogy with the corresponding force in classical fluids (inertial or pressure-gradient force), which depends on local fluid acceleration and includes the so-called Faxén corrections arising from velocity inhomogeneities close to the particle position [22]. The difference is that, in a classical fluid, these corrections arise from the finite size of the particle and vanish when the particle size becomes zero. In the BEC, Faxén-type corrections arise both from the particle size (modeled by the range of the particle repulsion potential) and from the BEC coherence length. As fluid-particle interaction becomes more important, a second contribution to the force becomes noticeable, which takes into account the drag on the particle arising from the perturbation of the flow produced by the presence of the particle. This is also called the particle *self-induced* force. We are able to obtain explicit formulae for the steady-state motion of the particle in an otherwise homogeneous and steady BEC. This drag is a dissipative (damping) force due to thermal drag of the BEC with the thermal cloud. It occurs in addition to the drag due to acoustic excitations in the condensate that occurs only above a critical velocity. It can be compared with the corresponding force in classical fluids, namely the viscous Stokes drag. We find an analytical expression for this self-induced drag at arbitrary speeds and show that in the low speed limit, it reduces to a linear dependence on speed akin to the classical Stokes drag.

The rest of the paper is structured as follows. In Sect. 2, we discuss the general modelling setup and in Sect. 3 a perturbation analysis is used to derive the linearised equations for the perturbations in the wavefunction related to non-steady condensate flow and the particle repulsive potential. Subsections 3.1 and 3.2 derive analytical expressions within perturbation theory for the two contributions to the force experienced by the particle. In Section 4, we compare our theoretical predictions with numerical simulations of the dissipative GPE coupled to the impurity, and the final section summarises our conclusions.

## 2. Modelling approach

We model the interaction between the impurity and a two-dimensional (2D) BEC through a Gaussian repulsive potential which can be reduced to a delta-function limit similar to previous studies [3, 5]. The BEC at low temperatures is well-described by the damped Gross Pitaevskii equation (dGPE) for the condensate wavefunction  $\psi(\mathbf{r}, t)$  [23, 24, 25, 26, 27, 28, 29]:

$$i\hbar\partial_t\psi = (1 - i\gamma) \left( -\frac{\hbar^2}{2m}\nabla^2 + g|\psi|^2 - \mu + V_{ext} + g_p\mathcal{U}_p \right) \psi, \quad (1)$$

where  $g$  is an effective scattering parameter between condensate atoms.  $V_{ext}$  is any external potential used to confine or stir the condensate. The damping coefficient  $\gamma > 0$  also called the thermal drag is related to the net exchange of atoms through collisions between thermal atoms with each other or with the condensate at fixed chemical potential  $\mu$ . In the low-temperature limit, this damping  $\gamma$  is very small and can be expressed as a function of temperature  $T$  [30, 25]. The dGPE is a phenomenological model that can also be derived from the stochastic GPE in the low temperature limit where noise is negligible [23, 24]. The dGPE has been used extensively to study different vortex regimes from vortex lattices [25] to quantum turbulence [28, 31, 27, 26, 32] and was shown to capture well, at least qualitatively, experimental observations [32].

A hydrodynamic description of the BEC uses the Madelung transformation of the wavefunction  $\psi = |\psi|e^{i\phi}$  to define the condensate density as  $\rho(\mathbf{r}, t) = |\psi(\mathbf{r}, t)|^2$  and the condensate velocity as  $\mathbf{v}(\mathbf{r}, t) = (\hbar/m)\nabla\phi(\mathbf{r}, t)$ . This velocity can also be obtained from the superfluid current  $\mathbf{J}(\mathbf{r}, t)$  as

$$\mathbf{J} = \frac{\hbar}{2mi} (\psi^*\nabla\psi - \psi\nabla\psi^*) = \rho\mathbf{v}, \quad (2)$$

where  $\psi^*$  denotes the complex conjugate of  $\psi$ . In addition to damping the BEC velocity, the presence of  $\gamma \neq 0$  in the dGPE also singles out the value  $\rho_h = |\psi|^2 = g/\mu$  as the steady homogeneous density value when the phase is constant and  $V_{ext} = 0$ .

The interaction potential  $\mathcal{U}_p(\mathbf{r} - \mathbf{r}_p)$  between the condensate and the impurity is modelled by a Gaussian potential  $\mathcal{U}_p(\mathbf{r} - \mathbf{r}_p) = \mu/(2\pi\sigma^2)e^{-(\mathbf{r}-\mathbf{r}_p)^2/(2\sigma^2)}$ . The parameter  $g_p > 0$  is the weak coupling constant for repulsive impurity-condensate interaction,  $\mathbf{r}_p = \mathbf{r}_p(t)$  denotes the center-of-mass position of the impurity, and  $\sigma$  its effective size. Here we consider an impurity of size  $\sigma$  of the order the coherence length  $\xi = \hbar/\sqrt{m\mu}$  of the condensate. The impurity is too small to nucleate vortices in its wake [33]. Instead, it will create acoustic excitations with Bogoliubov-Čerenkov wake. Similar wave fringes in the condensate density have been reported numerically in [2] for a different realisation of non-equilibrium Bose-Einstein condensates. In the limit of a point-like impurity, the Gaussian interaction potential converges to a two-body scattering potential  $\mathcal{U}_p(\mathbf{r}-\mathbf{r}_p, t) = \mu\delta(\mathbf{r}-\mathbf{r}_p(t))$  that has been used in previous analytical studies [3, 4, 13, 14]. Note that we are modelling only the interaction of the particle with the BEC, so that the viscous-like drag we obtain arises from the indirect coupling to the thermal bath via the BEC. Any direct interaction of the particle with the thermal cloud will lead to

additional forces which could be important at high temperatures, and which are not included here.

In order to gain insight into the forces and their relationship with the classical case, we keep the set-up as simple as possible. We consider a 2D condensate and assume that the size of the condensate is large enough so that we can neglect inhomogeneities in the confining part of  $V_{ext}$ . Also, we consider a neutrally buoyant impurity so that effects of gravity can be neglected. This would imply  $V_{ext} = 0$  except if an external forcing is introduced to stir the system, in which case we assume the support of this external force is sufficiently far from the impurity.

The impurity and the condensate will exert an interaction force on each other that is determined by the Ehrenfest theorem for the evolution of the center-of-mass momentum of the particle. The potential force  $-g_p \nabla \mathcal{U}_p(\mathbf{r} - \mathbf{r}_p)$  is the force exerted by an impurity on a condensate particle at position  $\mathbf{r}$ . By space averaging over condensate density, we then determine the force exerted by the impurity on the condensate as  $-g_p \int d\mathbf{r} |\psi(\mathbf{r}, t)|^2 \nabla \mathcal{U}_p(\mathbf{r} - \mathbf{r}_p)$  [14]. Hence, the force acting on the impurity has the opposite sign and is equal to

$$\mathbf{F}_p(t) = +g_p \int d^2\mathbf{r} |\psi(\mathbf{r}, t)|^2 \nabla \mathcal{U}_p(\mathbf{r} - \mathbf{r}_p) \quad (3)$$

which, through an integration by parts, is equivalent to

$$\mathbf{F}_p(t) = -g_p \int d^2\mathbf{r} \mathcal{U}_p(\mathbf{r} - \mathbf{r}_p, t) \nabla |\psi(\mathbf{r}, t)|^2. \quad (4)$$

Note that this last expression can also be used, reversing the sign, to give the force exerted on the BEC by a laser of beam profile given by  $\mathcal{U}_p$ .

At zero temperature, i.e.  $\gamma = 0$ , and if we neglect the effect of quantum fluctuations [17, 16, 18, 19], the impurity moves without any drag through a uniform condensate below a critical velocity, which is the low-wavelength speed of sound  $c = \sqrt{\mu/m}$ , as determined by the condensate linear excitation spectrum, in agreement with Landau's criterion of superfluidity [3]. Above the critical speed, the impurity will create excitations, and depending on the size of the impurity these excitations range from acoustic waves (Bogoliubov excitation spectrum) to vortex dipoles and to von-Karman street of vortex pairs [33]. Previous studies focused on the theoretical investigations of the self-induced drag force and energy dissipation rate in the presence of Bogoliubov excitations emitted by a pointwise [3, 16, 19] or finite-size [5] particle, or numerical investigations of the drag force due to vortex emissions [1, 13, 14]. The energy dissipation rate depends on whether the impurity is heavier, neutral or lighter with respect to the mass of the condensate particles [14]. The dependence on the velocity of the self-induced drag force above the critical velocity changes with the spatial dimensions [3]. This means that the energy dissipation rate is also dependent on the spatial dimensions. If instead of a single impurity one considers many of them there will be, besides direct inter-particle interactions, additional forces between the impurities mediated by the flow, leading to a much more complex many-body dynamics even in an otherwise uniform condensate,

as discussed in [4]. Here we neglect all these effects and consider a single impurity in a 2D BEC.

We rewrite the dGPE in dimensionless units by using the characteristic units of space and time in terms of the long-wavelength speed of sound  $c = \sqrt{\mu/m}$  in the homogeneous condensate and the coherence length  $\xi = \hbar/(mc) = \hbar/\sqrt{m\mu}$ . Space is rescaled as  $\mathbf{r} \rightarrow \tilde{\mathbf{r}}\xi$  and time as  $t \rightarrow \tilde{t}\xi/c$ . In addition, the wavefunction is also rescaled  $\psi \rightarrow \tilde{\psi}\sqrt{\mu/g}$ , where  $g/\mu$  is the equilibrium particle-number density corresponding to the solution with constant phase if  $V_{ext}, \mathcal{U}_p = 0$ . The external potential,  $V_{ext} = \mu\tilde{V}_{ext}$ , and the interaction potential,  $g_p\mathcal{U}_p = \mu\tilde{g}_p\tilde{\mathcal{U}}_p$ , are measured in units of the chemical potential  $\mu$  with  $\tilde{\mathcal{U}}_p = 1/(2\pi a^2)e^{-(\tilde{r}-\tilde{r}_p)^2/(2a^2)}$ , and  $a = \sigma/\xi$ ,  $\tilde{g}_p = g_p/(\xi^2\mu)$ . Henceforth, the dimensionless form of the dGPE reads as

$$\partial_t \tilde{\psi} = (i + \gamma) \left( \frac{1}{2} \tilde{\nabla}^2 + 1 - \tilde{V}_{ext} - \tilde{g}_p \tilde{\mathcal{U}}_p - |\tilde{\psi}|^2 \right) \tilde{\psi}. \quad (5)$$

In these dimensionless units, the force from Eq. (4) exerted on an impurity reads as  $\mathbf{F}_p = (\mu^2\xi/g)\tilde{\mathbf{F}}_p$ , where

$$\tilde{\mathbf{F}}_p(t) = -\tilde{g}_p \int d^2\tilde{\mathbf{r}} \tilde{\mathcal{U}}_p(\mathbf{r} - \mathbf{r}_p) \tilde{\nabla} |\tilde{\psi}(\tilde{\mathbf{r}}, t)|^2. \quad (6)$$

For the rest of the paper, we will now omit the tildes over the dimensionless quantities.

In the limit of a point-like particle,  $\mathcal{U}_p = \delta(\mathbf{r} - \mathbf{r}_p)$ , the force from Eq. (6) becomes

$$\mathbf{F}_p(t) = -g_p \nabla |\psi(\mathbf{r}, t)|^2|_{\mathbf{r}=\mathbf{r}_p(t)}. \quad (7)$$

### 3. Perturbation analysis

For a weakly-interacting impurity, the condensate wavefunction  $\psi$  can be decomposed into an unperturbed wavefunction  $\psi_0(\mathbf{r})$  describing the motion and density of the fluid in the absence of the particle and the perturbation  $\delta\psi_1(\mathbf{r})$  due to the impurity's repulsive interaction with the condensate, hence  $\psi = \psi_0 + g_p\delta\psi_1$ . Weak particle-condensate interaction condition is that  $\max(g_p\mathcal{U}_p) \ll 1$ , or  $g_p \ll 2\pi a^2$ , which means that the particle-condensate interaction of strength  $g_p$  and range  $\sigma$  is small compared with the energy scale given by the chemical potential  $\mu = 1$  (dimensionless units).

The unperturbed wavefunction  $\psi_0(\mathbf{r}, t)$  can be spatially-dependent, if it is initialised in a nonequilibrium configuration, or if external forces characterised by  $V_{ext}$  are at play. Here, we consider deviations with respect to the steady and uniform equilibrium state ( $\psi_h = 1$  in dimensionless units). As stated before, we do not consider large extended inhomogeneities produced by a trapping potential, and assume that any stirring force acting on the BEC is far from the particle. Thus, we treat inhomogeneities close to the particle as small perturbations to the uniform state  $\psi_h = 1$ :  $\psi_0(\mathbf{r}, t) = 1 + \delta\psi_0(\mathbf{r}, t)$ . Combining the two types of perturbations, and using the relationships of the wavefunction to the density, velocity and current (Eq. (2), which in dimensionless units reads  $\rho\mathbf{v} = (\psi^*\nabla\psi - \psi\nabla\psi^*)/(2i)$ ) we find

$$\psi = 1 + \delta\psi_0 + g_p\delta\psi_1 \quad (8)$$

$$\rho = 1 + \delta\rho_0 + g_p\delta\rho_1, \quad (9)$$

$$\mathbf{v} = \delta\mathbf{v}^{(0)} + g_p\delta\mathbf{v}^{(1)}, \quad (10)$$

where

$$\delta\rho_0 = \delta\psi_0 + \delta\psi_0^*, \quad \delta\rho_1 = \delta\psi_1 + \delta\psi_1^*, \quad (11)$$

$$\delta\mathbf{v}^{(0)} = \frac{1}{2i}\nabla(\delta\psi_0 - \delta\psi_0^*), \quad \delta\mathbf{v}^{(1)} = \frac{1}{2i}\nabla(\delta\psi_1 - \delta\psi_1^*). \quad (12)$$

Combining Eq. (6) with the expressions for the density perturbations, we have that the total force can be split into the contribution from the density variations in the BEC by causes external to the particle (initial preparation, stirring forces in  $V_{ext}$ , ...), and the density perturbations due to the presence of the particle  $\mathbf{F}_p = \mathbf{F}^{(0)} + \mathbf{F}^{(1)}$ :

$$\mathbf{F}^{(0)}(t) = -\frac{g_p}{2\pi a^2} \int d^2\mathbf{r} e^{-\frac{(\mathbf{r}-\mathbf{r}_p(t))^2}{2a^2}} \nabla\delta\rho_0(\mathbf{r}, t), \quad (13)$$

$$\mathbf{F}^{(1)}(t) = -\frac{g_p^2}{2\pi a^2} \int d^2\mathbf{r} e^{-\frac{(\mathbf{r}-\mathbf{r}_p(t))^2}{2a^2}} \nabla\delta\rho_1(\mathbf{r}, t). \quad (14)$$

The perturbative splitting of the force in these two contributions is completely analogous to the corresponding classical-fluid case in the incompressible [22] and in the compressible [34] situations. The  $\mathbf{F}^{(0)}$  contribution is the equivalent to the classical inertial or pressure-gradient force on a test particle, which does not disturb the fluid, in a inhomogeneous and unsteady flow. We call this the *inertial* force. The  $\mathbf{F}^{(1)}$  contribution takes into account perturbatively the modifications on the flow induced by the presence of the particle, and it is called the *self-induced drag* on the particle. To complete the comparison with the classical expressions [22, 34], we need to express Eqs. (13) and (14) in terms of the unperturbed velocity field  $\mathbf{v}^{(0)}(\mathbf{r}, t) = \delta\mathbf{v}^{(0)}(\mathbf{r}, t)$  and of the particle speed  $\mathbf{V}_p(t) = \dot{\mathbf{r}}_p(t)$ . We are able to do so in a general situation for the inertial force  $\mathbf{F}^{(0)}$ . For  $\mathbf{F}^{(1)}$ , we obtain analytical expressions in the simple case where the impurity is moving with a constant velocity in an otherwise uniform BEC.

The desired relationships between  $\nabla\delta\rho_0$  and  $\nabla\delta\rho_1$  in Eqs. (13)-(14), and  $\delta\mathbf{v}^{(0)}$  and  $\mathbf{V}_p$  will be obtained from the linearization of the dGPE Eq. (5) around the uniform steady state  $\psi_h = 1$ :

$$\partial_t\delta\psi_0 = (i + \gamma) \left( \frac{1}{2}\nabla^2 - 1 \right) \delta\psi_0 - (i + \gamma)\delta\psi_0^*, \quad (15)$$

$$\partial_t\delta\psi_1 = (i + \gamma) \left( \frac{1}{2}\nabla^2 - 1 \right) \delta\psi_1 - (i + \gamma)\delta\psi_1^* - (i + \gamma)\mathcal{U}_p(\mathbf{r} - \mathbf{r}_p). \quad (16)$$

Terms containing  $V_{ext}$  are not included in Eq. (15) because of our assumption of sufficient distance between possible stirring sources and the neighborhood of the particle position, the only region that—as we will see—will enter into the calculation of the forces. In the next sections we solve these linearised equations to relate density perturbations to undisturbed velocity field and particle velocity.

### 3.1. Inertial force

To convert Eq. (13) for the inertial force into an expression suitable for comparison with the corresponding term in classical fluids, we need to express  $\nabla\delta\rho_0$  in terms of the undisturbed velocity field  $\mathbf{v}^{(0)}(\mathbf{r}, t) = \delta\mathbf{v}^{(0)}(\mathbf{r}, t)$ . To this end, we subtract Eq. (15) from its complex conjugate, obtaining:

$$(\nabla^2 - 4) \nabla\delta\rho_0 = 4 \left( \partial_t - \frac{\gamma}{2} \nabla^2 \right) \delta\mathbf{v}^{(0)}, \quad (17)$$

where we have used Eqs. (11) and (12). Since the force formulae require to obtain the condensate density in a neighbourhood of the particle position, it is convenient to move to frame co-moving with the particle. Thus we change variables from  $(\mathbf{r}, t)$  to  $(\mathbf{z}, t)$ , with  $\mathbf{z} = \mathbf{r} - \mathbf{r}_p(t)$ , and the velocity field will be now referred to the particle velocity  $\mathbf{V}_p(t) = \dot{\mathbf{r}}_p(t)$ :  $\delta\mathbf{w}^{(0)}(\mathbf{z}, t) = \delta\mathbf{v}^{(0)}(\mathbf{r}, t) - \mathbf{V}_p(t)$ . Equation (17) becomes:

$$(\nabla_z^2 - 4) \nabla_z\delta\rho_0 = 4 \left( \partial_t - \mathbf{V}_p \cdot \nabla_z - \frac{\gamma}{2} \nabla_z^2 \right) \delta\mathbf{w}^{(0)} + \dot{\mathbf{V}}_p(t), \quad (18)$$

which has the corresponding equation for its Green's function given by

$$(\nabla_z^2 - 4) G(\mathbf{z}) = \delta(\mathbf{z}) \quad (19)$$

with the boundary condition  $G(|\mathbf{z}| \rightarrow \infty) \rightarrow 0$  (corresponding to vanishing  $\nabla_z\delta\rho_0(\mathbf{r})$  at  $|\mathbf{r}| = \infty$ ). The solution is given by the zeroth order modified Bessel function  $G(\mathbf{z}) = -K_0(2|\mathbf{z}|)/(2\pi)$ . Hence, the gradient of the density perturbation can be written as the convolution with the Green's function:

$$\nabla_z\delta\rho_0(\mathbf{z}, t) = -\frac{2}{\pi} \int d\mathbf{z}' K_0(2|\mathbf{z}-\mathbf{z}'|) \left[ \left( \partial_t - \mathbf{V}_p \cdot \nabla_{\mathbf{z}'} - \frac{\gamma}{2} \nabla_{\mathbf{z}'}^2 \right) \delta\mathbf{w}^{(0)}(\mathbf{z}', t) + \dot{\mathbf{V}}_p(t) \right], \quad (20)$$

and the expression for the force (13), using the comoving variables  $(\mathbf{z}, t)$ , becomes:

$$\mathbf{F}^{(0)}(t) = -\frac{g_p}{\pi^2 a^2} \int d\mathbf{z} e^{-\frac{z^2}{2a^2}} \int d\mathbf{z}' K_0(2|\mathbf{z}-\mathbf{z}'|) \left[ \left( \partial_t - \mathbf{V}_p \cdot \nabla_{\mathbf{z}'} - \frac{\gamma}{2} \nabla_{\mathbf{z}'}^2 \right) \delta\mathbf{w}^{(0)}(\mathbf{z}', t) + \dot{\mathbf{V}}_p(t) \right]. \quad (21)$$

The above expression is a weighted average of contributions from properties of the fluid velocity in a neighborhood of the impurity center-of-mass position ( $\mathbf{z} = 0$  in the comoving frame). The size of this neighborhood is given by the combination of the range of the Bessel function kernel, which in dimensional units would be the correlation length  $\xi$ , and the range of the Gaussian potential,  $a$ , giving an effective particle size. In classical fluids, the analogous force on a spherical particle involves the average of properties of the undisturbed velocity field within the sphere size [34], and there is no equivalent to the role of  $\xi$ .

As in the classical case [22, 34], if fluid velocity variations are weak at scales below  $a$  and  $\xi$ , we can approximate the condensate velocity by a Taylor expansion near the impurity, i.e.:

$$\delta w_i^{(0)}(\mathbf{z}', t) \approx \delta w_i^{(0)}(t) + \sum_j e_{ij}(t) z'_j + \frac{1}{2} \sum_{jk} e_{ijk}(t) z'_j z'_k + \dots, \quad (22)$$

where the indices  $i, j, k = x, y$  denote the coordinate components.  $e_{ij}(t) = \partial_j \delta w_i^{(0)}(\mathbf{z}, t)|_{\mathbf{z}=0}$  and  $e_{ijk}(t) = \partial_j \partial_k \delta w_i^{(0)}(\mathbf{z}, t)|_{\mathbf{z}=0}$  are gradients of the unperturbed

condensate relative velocity. Inserting this expansion into Eq. (21), and performing the integrals of the Gaussian and of the Bessel function (using for example  $\int K_0(2|z|)dz = \pi/2$  and  $\int z_i z_j K_0(2|z|)dz = (\delta_{ij}/2) \int_0^\infty 2\pi z^3 K_0(2z)dz = \delta_{ij}\pi/4$ ), we obtain:

$$\mathbf{F}^{(0)}(t) \approx g_p \dot{\mathbf{V}}_p(t) + g_p \left[ \partial_t - \mathbf{V}_p(t) \cdot \nabla_z + \frac{a^2}{2} \partial_t \nabla_z^2 - \frac{\gamma}{2} \nabla_z^2 + \frac{1}{4} \partial_t \nabla_z^2 \right] \delta \mathbf{w}^{(0)}(\mathbf{z}, t)|_{\mathbf{z}=\mathbf{0}}. \quad (23)$$

The terms containing Laplacians are analogous to the Faxén corrections in classical fluids [22] which arise for particles with finite size. Here, they arise from a combination of the finite effective size of the particle,  $a$ , and of the quantum coherence length,  $\xi = 1$ . This last effect remains even in the limit of vanishing particle size  $a \rightarrow 0$ . Interestingly, one of the two terms in these quantum corrections depend on  $\gamma$  hence indirectly on the presence of the thermal cloud.

As in the classical case, if flow inhomogeneities are unimportant below the scales  $a$  and  $\xi$ , we can neglect the Laplacian terms in Eq. (23). Returning to the variables  $(\mathbf{r}, t)$  in the lab frame of reference, the terms containing  $\mathbf{V}_p$  cancel out, showing that the inertial force is mainly given by the local fluid acceleration:

$$\mathbf{F}^{(0)}(t) = g_p \partial_t \delta \mathbf{v}^{(0)}(\mathbf{r}, t)|_{\mathbf{r}=\mathbf{r}_p(t)}. \quad (24)$$

We have assumed a small non-uniform unperturbed velocity field  $\mathbf{v}^{(0)}(\mathbf{r}, t) = \delta \mathbf{v}^{(0)}(\mathbf{r}, t)$ . To leading order in velocity, the partial derivative  $\partial_t \delta \mathbf{v}^{(0)}$  and the material derivative  $D\delta \mathbf{v}^{(0)}/Dt = \partial_t \delta \mathbf{v}^{(0)} + \delta \mathbf{v}^{(0)} \cdot \nabla \delta \mathbf{v}^{(0)}$  are identical. In classical fluids the same ambiguity occurs and it has been established, on physical grounds and by going beyond linearisation, that using the material derivative is more correct [22]. After all, using this material derivative in the equation of motion simply means that, under the above approximations and in places where stirring and other external forces are absent, the local acceleration on the impurity arises from the corresponding acceleration of the condensate. Since for  $a \rightarrow 0$  the condensate-impurity interaction has a similar scattering potential (delta function) as that for the interaction between condensate particles, similar accelerations would be experienced by a condensate particle and by the impurity, just modulated by a different coupling constant. Thus, replacing  $\partial_t$  by  $D/Dt$  in (24) the approximate inertial force becomes:

$$\mathbf{F}^{(0)}(t) = g_p \left. \frac{D\mathbf{v}^{(0)}}{Dt} \right|_{\mathbf{r}=\mathbf{r}_p(t)}, \quad (25)$$

or, if we return back to dimensional variables:

$$\mathbf{F}^{(0)}(t) = \frac{g_p}{g} m \left. \frac{D\mathbf{v}^{(0)}}{Dt} \right|_{\mathbf{r}=\mathbf{r}_p(t)}. \quad (26)$$

This is equivalent to the equation for the inertial force in classical fluids [22] except that the coefficient of the material derivative in the classical case is the mass of the fluid fitting in the size of the impurity. In the comoving frame, replacement of the partial by the material derivative amounts to replace  $(\partial_t - \mathbf{V}_p \cdot \nabla_{z'}) \delta \mathbf{w}^{(0)}$  in Eq. (21) by  $D\delta \mathbf{w}^{(0)}/Dt$ . Eq. (25) is expected to be valid for small values of  $g_p$  and in regions where fluid velocity and density inhomogeneities are both small and weakly varying. At this

level of approximation neither compressibility nor dissipation effects appear explicitly in the inertial force, in analogy with classical compressible fluids [34]. But these effects are indirectly present by determining the structure of the field  $\mathbf{v}^{(0)}(\mathbf{r}, t)$ .

### 3.2. Self-induced drag force

The consideration of the self-induced force on a particle moving through a classical fluids leads to different terms, namely [22, 34] the viscous (Stokes) drag, the unsteady-inviscid term that in the incompressible case becomes the added-mass force, and the unsteady-viscous term that in the incompressible case becomes the Basset history force. They are expressed in terms of the undisturbed velocity flow  $\mathbf{v}^{(0)}$  and the particle velocity  $\mathbf{V}_p(t)$ . Here, for the BEC case, we are able to obtain the self-induced force only for a particle moving at constant speed on the condensate. For the classical fluid case, in this situation the only non-vanishing force is the Stokes drag, so that this is the force we have to compare our result with. We note that the condensate itself in the absence of the particle perturbation can be in any state of (weak) motion since in our perturbative approach summarised in Eqs (15)-(16), the inhomogeneity  $\delta\psi_0$  and the  $g_p$ -perturbation  $\delta\psi_1$  are uncoupled.

It is convenient to transform the problem to the co-moving frame  $(\mathbf{r}, t) \rightarrow (\mathbf{z}, t)$  with  $\mathbf{z} = \mathbf{r} - \mathbf{r}_p(t)$ , so that Eq. (16) becomes

$$\partial_t \delta\psi_1 - \mathbf{V}_p \cdot \nabla \delta\psi_1 = (i + \gamma) \left( \frac{1}{2} \nabla^2 - 1 \right) \delta\psi_1 - (i + \gamma) \delta\psi_1^* - (i + \gamma) \mathcal{U}(\mathbf{r}). \quad (27)$$

Note that such Galilean transformations of the GPE using a constant  $\mathbf{V}_p$  are often accompanied by a multiplication of the transformed wavefunction by a phase factor  $\exp(i\mathbf{V}_p \cdot \mathbf{z} + \frac{i}{2} V_p^2 t)$ , in order to transform the condensate velocity (see below) to the new frame of reference, and account for the shift in kinetic energy. Indeed, such a combined transformation leaves the GPE unchanged at  $\gamma = 0$  [35] (but not for  $\gamma > 0$ ). The density perturbation  $\delta\rho_1$  is already given correctly by  $\delta\psi_1 + \delta\psi_1^*$ , where  $\delta\psi_1(\mathbf{z}, t)$  is the solution of (27), without the need of any additional phase factor. The velocity in the co-moving frame would need to be corrected as  $\delta\omega^{(1)}(\mathbf{z}, t) = \delta\mathbf{v}^{(1)} - \mathbf{V}_p$ , with  $\delta\mathbf{v}^{(1)}$  given by Eq. (12) in terms of the solution of Eq. (27).

Eq. (27) in the steady-state can be solved by using the Fourier transform  $\delta\psi_1(\mathbf{z}) = 1/(2\pi)^2 \int d^2\mathbf{k} e^{i\mathbf{k} \cdot \mathbf{z}} \delta\hat{\psi}_1(\mathbf{k})$ . It follows that the linear system of equations for  $\delta\hat{\psi}_1(\mathbf{k})$  and  $\delta\hat{\psi}_1^*(-\mathbf{k})$  is given by

$$\begin{aligned} [-2i\mathbf{k} \cdot \mathbf{V}_p + (i + \gamma)(k^2 + 2)] \delta\hat{\psi}_1 + 2(i + \gamma)\delta\hat{\psi}_1^* &= -2(i + \gamma)e^{-\frac{a^2 k^2}{2}}, \\ [-2i\mathbf{k} \cdot \mathbf{V}_p + (-i + \gamma)(k^2 + 2)] \delta\hat{\psi}_1^* + 2(-i + \gamma)\delta\hat{\psi}_1 &= -2(-i + \gamma)e^{-\frac{a^2 k^2}{2}}. \end{aligned} \quad (28)$$

By solving these equations, we find  $\delta\hat{\psi}_1(\mathbf{k})$  and  $\delta\hat{\psi}_1^*(-\mathbf{k})$ , and the Fourier transform of the density perturbation  $\delta\rho_1 = \delta\psi_1^* + \delta\psi_1$  then follows as

$$\delta\hat{\rho}_1 = \frac{e^{-\frac{k^2 a^2}{2}} (4k^2(1 + \gamma^2) - 8i\gamma\mathbf{k} \cdot \mathbf{V}_p)}{4\mathbf{k} \cdot \mathbf{V}_p (\mathbf{V}_p \cdot \mathbf{k} + i\gamma k^2 + 2i\gamma) - k^2(4 + k^2)(1 + \gamma^2)}. \quad (29)$$

Using the convolution theorem, we can express the self-induced force (14) (in the co-moving frame, i.e. with  $\mathbf{r}_p = 0$ ) in terms of  $\delta\hat{\rho}_1$  as

$$\mathbf{F}^{(1)} = -\frac{g_p^2}{(2\pi)^2} \int d^2\mathbf{k} i\mathbf{k} \delta\hat{\rho}_1(\mathbf{k}) e^{-\frac{k^2 a^2}{2}}. \quad (30)$$

This force can be decomposed into the normal and tangential components relative to the particle velocity  $\mathbf{V}_p$ :  $\mathbf{F}^{(1)} = F_{\parallel} \mathbf{e}_{\parallel} + F_{\perp} \mathbf{e}_{\perp}$ . Due to symmetry, the normal component vanishes upon polar integration, and we are left with the tangential, or drag, force

$$F_{\parallel} = -\frac{g_p^2}{(2\pi)^2} \int_0^{\infty} dk \int_0^{2\pi} d\theta e^{-k^2 a^2} \frac{ik^2 \cos(\theta) [4k^2(1 + \gamma^2) - 8i\gamma k V_p \cos(\theta)]}{4k V_p \cos(\theta) (k V_p \cos(\theta) + i\gamma k^2 + 2i\gamma) - k^2(4 + k^2)(1 + \gamma^2)}. \quad (31)$$

$V_p$  is the modulus of  $\mathbf{V}_p$ . At zero temperature, i.e. when  $\gamma = 0$ , the drag force reduces to the one that has also been calculated for a point particle in Refs. [3] and in [5] for a finite- $a$  particle:

$$F_{\parallel} = -\frac{g_p^2}{\pi^2} \int_0^{\infty} dk \int_0^{2\pi} d\theta \frac{ik^2 \cos \theta e^{-k^2 a^2}}{4V_p^2 \cos^2 \theta - (4 + k^2)}, \quad (32)$$

which is zero for particle speed smaller than the critical value given by the long-wavelength sound speed,  $V_p < c = 1$ . Above the critical speed, the integral has poles and acquires a non-zero value given by

$$F_{\parallel} = -\frac{g_p^2 k_{max}^2}{4V_p} e^{-\frac{a^2 k_{max}^2}{2}} \left[ I_0 \left( \frac{a^2 k_{max}^2}{2} \right) - I_1 \left( \frac{a^2 k_{max}^2}{2} \right) \right] \quad (33)$$

in terms of the modified Bessel functions of the first kind  $I_n(x)$  and where  $k_{max} = 2\sqrt{V_p^2 - 1}$ . For vanishing  $a$  the dominant term is proportional to  $(V_p^2 - 1)/V_p$  [3]. This drag is pertaining to energy dissipation by radiating sound waves in the condensate away from the impurity. We emphasise again that  $a$  is small enough such that emission of other excitations, such as vortex pairs, does not occur. It is important to note [3, 5] that in order to obtain a real value for the force in Eq. (33) one has to consider that it has been obtained from the limit  $\gamma \rightarrow 0^+$  in (31), which implies that an infinitesimal positive imaginary part needs to be considered in the denominator to properly deal with the poles in the integral.

In general, for a non-zero  $\gamma$ , Eq. (31) simplifies upon an expansion in powers of  $V_p$  to the leading order. For the linear term in  $V_p$ , we can perform the polar integration and arrive at

$$F_{\parallel} = -\frac{2}{\pi} V_p \frac{\gamma}{1 + \gamma^2} g_p^2 \int \frac{k^3 e^{-a^2 k^2}}{(4 + k^2)^2} dk. \quad (34)$$

Substituting  $u = a^2(k^2 + 4)$ , we find

$$F_{\parallel} = -V_p \frac{\gamma}{1 + \gamma^2} g_p^2 \frac{1}{\pi} \left[ e^{4a^2} E_1(4a^2)(1 + 4a^2) - 1 \right], \quad (35)$$

where  $E_1(x)$  denotes the positive exponential integral. When  $a \rightarrow 0$ , the expression inside the bracket diverges as  $-\gamma_E - 1 - \ln(4a^2)$  with  $\gamma_E$  begin the Euler-Mascheroni constant. It is therefore necessary to keep a finite size  $a$ .

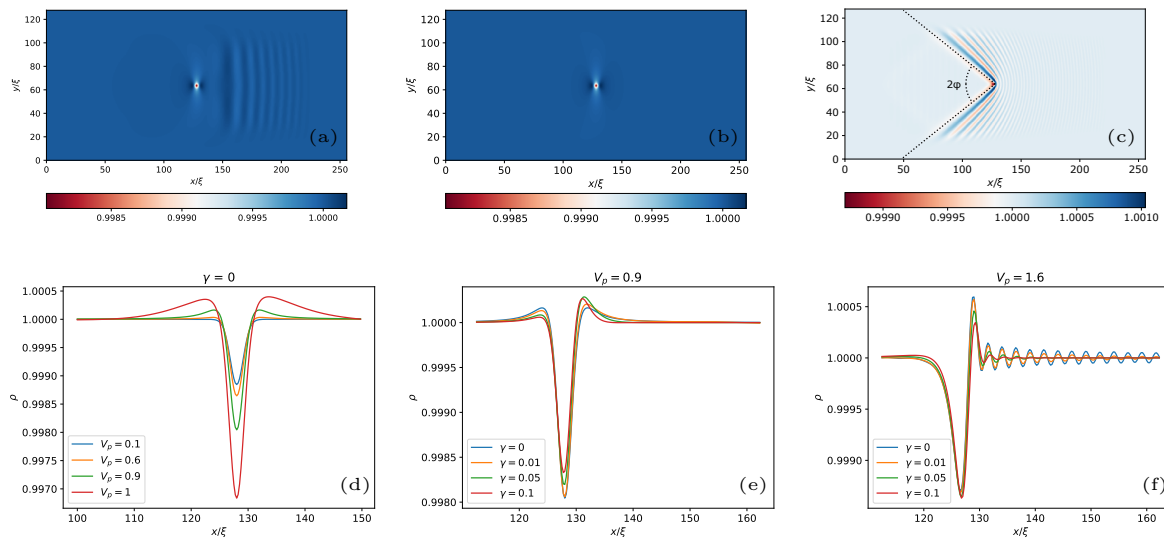


**Figure 1.** Panels (a)-(c) show 2D snapshots of the condensate density for  $\gamma = 0$ . The impurity is at  $x/\xi = 128$  and  $y/\xi = 64$ . (a) is at  $V_p = 0.9$  and at time  $t = 200$ , with transient waves still in the system. (b) is for the same  $V_p = 0.9$  and at  $t = 2000$ , when the final steady state has been reached. Panel (c) is for  $V_p = 1.6 > 1$ , for which some waves remain attached to the impurity as front fringes and the Bogoliubov-Čerenkov wake with  $\sin(\phi) = 1/V_p$ . Panels (d-f) show cross-section profiles along the  $x$  direction of the steady-state condensate density around the impurity. Panel (d) shows the front-rear symmetry of the steady profiles when  $V_p \leq 1$  and  $\gamma = 0$ . An asymmetry develops (panel (e)) for  $\gamma > 0$ , which relates to the net viscous-like drag. Panel (f) displays density profiles for  $V_p = 1.6 > 1$  and different values of  $\gamma$ . The asymmetric density profile corresponds to waves trapped in front of the moving particle. With increasing  $\gamma$ , these waves are damped out.

This drag force is akin to the viscous Stokes drag in classical fluids, but it is due to loss of energy in the condensate through its interaction with the thermal cloud. The effective drag coefficient depends on the thermal drag such that it vanishes at zero temperature. But it also depends non-trivially on the size of the impurity and it diverges in the limit of point-like particle. Faxén corrections involving derivatives of the unperturbed flow are not present here because of the decoupling between  $\delta\psi_0$  and  $\delta\psi_1$  arising in the perturbative approach leading to (15)-(16).

#### 4. Numerical results

To test the analytical predictions of the inertial force and the self-induced drag deduced above from the total force expression Eq. (6), we performed numerical simulations of the dGPE. Actually, our simulations are done in the co-moving frame of the impurity moving at constant velocity  $\mathbf{V}_p$ , so that the equation we solve is (see numerical details

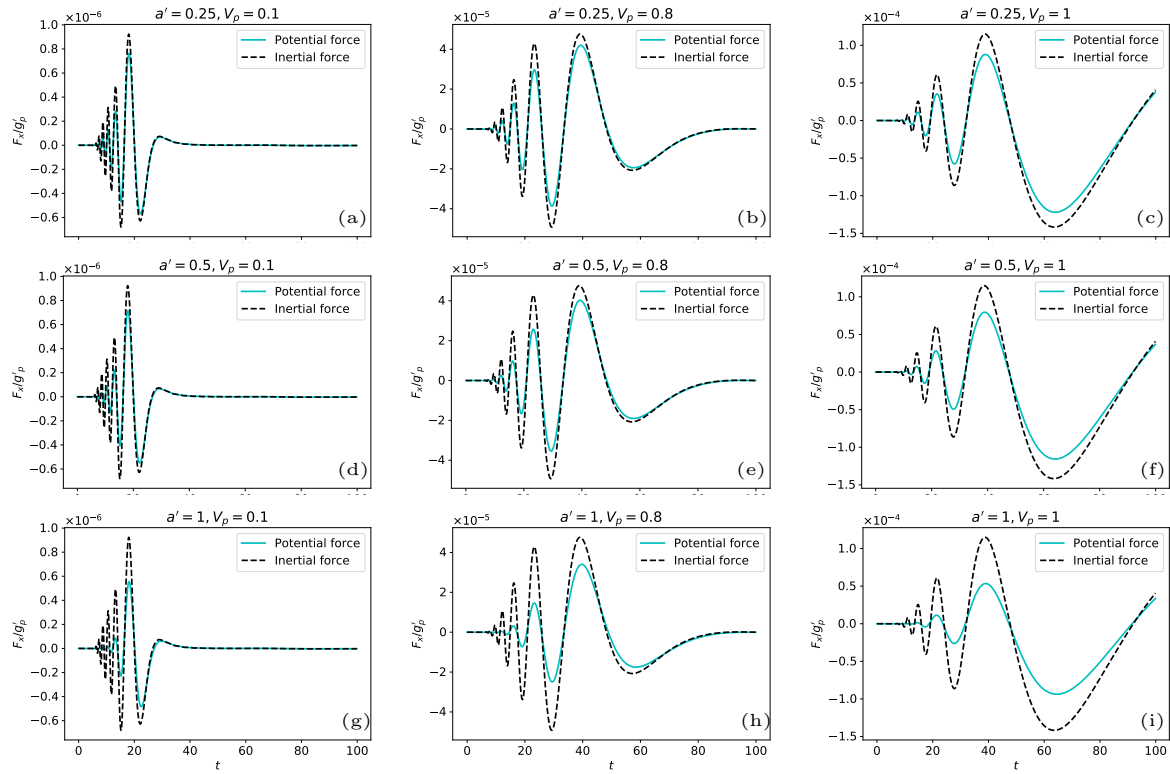


**Figure 2.**  $x$  component of the time-dependent force  $F_x/g'_p$ , using direct numerical simulations of the dGPE Eq. (36), on a test particle of size  $a' = 0.25, 0.5, 1$  at a relative position  $(\Delta x, \Delta y) = (10, 20)$  with respect to the position of the particle producing the flow perturbation. The speed of both particles is  $V_p = 0.1, 0.8, 1$ , and  $\gamma = 0$ . Cyan continuous lines correspond to the full force ( $x$  component) from the exact expression Eq. (6). They are labeled as ‘potential force’ because of the rather explicit appearance of the interaction potential in this formula. Black dotted lines are the predictions for the inertial force from the approximation Eq. (25) (computed in the comoving frame as explained in the text).

in the Appendix):

$$\partial_t \psi - \mathbf{V}_p \cdot \nabla \psi = (i + \gamma) \left[ \frac{1}{2} \nabla^2 \psi + (1 - g_p \mathcal{U}_p - |\psi|^2) \psi \right], \quad (36)$$

where the impurity is described by the Gaussian potential of intensity  $g_p = 0.01$  and effective size  $a = 1$  (in units of  $\xi$ ), and is situated in the middle of the domain with the coordinates  $(x, y) = (128, 64)$  (in units of  $\xi$ ). As an initial condition, we start with the condensate being at rest and in equilibrium with the impurity. This is done by imaginary time integration of Eq. (36) for  $V_p = 0$  and  $\gamma = 0$ . Then, at  $t = 0$ , we solve the full Eq. (36), and as a consequence, sound waves are emitted from the neighbourhood of the impurity. Their speed is determined by the dispersion relation  $\omega(\mathbf{k})$  giving the frequency as a function of the wavenumber and can be obtained by looking for plane-wave solutions to Eq. (15). If  $\gamma = 0$ ,  $\omega(\mathbf{k})$  is given by the Bogoliubov dispersion relation [36]  $\omega(\mathbf{k}) = k\sqrt{1 + k^2/4}$ . Note that the smallest velocity,  $c = 1$ , is that of long wavelengths, and that waves of smaller wavelength travel faster. For

$\gamma > 0$ , the planar waves are dampened out and the dispersion relation becomes  $\omega(\mathbf{k}) = -i\gamma(k^2/2 + 1) + \sqrt{k^2 + k^4/4 - \gamma^2}$ . The damping rate is determined by  $\gamma$  and increases quadratically with the wavenumber. Also, in this case all waves have a group velocity faster than a minimum one that for small  $\gamma$  is close to  $c = 1$ .

When  $V_p < 1$  all the waves escape the neighbourhood of the impurity (see an example in Fig. 1(a)) and are dissipated in a boundary buffer region that has large  $\gamma$  (see numerical details in the Appendix and Supplementary Material [37]). After a transient the condensate achieves a steady state. Fig. 1(b) shows a steady spatial configuration for  $\gamma = 0$  and  $V_p = 0.9$ . Figs. 1(d-e) show different profiles of the condensate density along the  $x$  direction across the impurity position for  $V_p$ . The condensate density is depleted near the impurity due to the repulsive interaction, and its general shape depends on the speed  $V_p$  and thermal drag  $\gamma$ . If  $\gamma = 0$  and  $V_p \leq 1$  the density of this steady state has a rear-front symmetry with respect to the particle position (see specially Fig. 1(d)), so that under integration in Eq. (6) the net force is zero. The presence of dissipation ( $\gamma > 0$ ) breaks this symmetry even if  $V_p < 1$  so that a net drag will appear in agreement with the calculation of Sect. 3.2. When  $V_p > 1$ , there are waves that can not escape from the neighbourhood of the impurity, forming parabolic fringes in front of it and the Bogoliubov-Čerenkov wake behind it. (see Fig. 1(c) and 1(f) and Supplemental material [37]). The opening angle of the Čerenkov cone is determined by the dispersion relation of the waves with long-wavelength and satisfy the relation  $\sin(\phi) = 1/V_p$  as shown in Fig. 1(c). It is clear that it narrows when the speed increases. The consequence is that there is a net drag induced by these fringes even when  $\gamma = 0$ , and that it would eventually decrease at very large velocity as the angle of the wake decreases. Similar gringes in the condensate density around an obstacle in supersonic flows has also been observed experimentally [38]. Movies showing the transient and long-time density behaviour for several values of  $V_p$  and at  $\gamma = 0$  are included as Supplemental Material [37]. The fluid suddenly starts to move towards the negative  $x$  direction, and its density approaches a steady state after the transient. Note that during all the dynamics, the density deviation with respect to the equilibrium value  $\rho = 1$  is very small, justifying the perturbative approach of Sect. 3. The time evolution for  $\gamma > 0$  is qualitatively similar to the  $\gamma = 0$  shown in the movies, except that the waves become damped and that there is a front-rear asymmetry in the steady state.

Our numerical setup is well suited to measure the force produced by the perturbation of the impurity on the fluid, i.e. the self-induced drag. Nevertheless, in the absence of the impurity the unperturbed state is the trivial  $\psi = 1$ , so that  $\delta\psi_0 = 0$  and the inertial force is identically zero. In order to test the accuracy of our expressions for the inertial force without the need of additional simulations under a different set-up, we still use the computed condensate density and velocity dynamics, produced by the impurity introduced in the system at  $t = 0$ , but we evaluate the inertial force exerted by this flow on another test particle located at a different position. In fact, there is no need to think on the flow as being produced by an impurity: it can be produced by a moving laser beam that can modelled by an external potential  $V_{ext}$  and the only impurity present

in the system is the test particle on which the force is evaluated. In the following we evaluate the inertial and the self-induced drag forces on the different particles from the general expressions Eqs. (13)-(14) and from the approximate expressions of Sects. 3.1 and 3.2.

#### *4.1. Numerical evaluation of the inertial force*

We consider a test particle traveling at the same speed  $V_p$  as the impurity or laser beam producing the flow, but located at a distance of 10 coherence lengths in front of it, and 20 coherence lengths in the  $y$  direction apart from it. This distance is sufficient to avoid inclusion of  $\mathcal{U}_p$  or  $V_{ext}$  in Eq. (15) for the neighborhood of the test particle. Condensate and test particle interact via a coupling constant  $g'_p$  sufficiently small so that the full force on the later, Eq. (6), is well approximated by the inertial part Eq. (13), being the perturbation the particle induces on the flow, and thus the force (14) completely negligible.

Figure (2) shows, for different values of  $V_p = 0.1, 0.8, 1$  at  $\gamma = 0$ , the  $x$  component of the time-dependent force produced by the transient flow inhomogeneities hitting the test particle in the form of sound waves. The size of the test particle, taking several values, is called  $a'$  to distinguish it from the size  $a$  of the particle producing the flow perturbation. Blue lines are computed from the exact Eq. (6) or equivalently from Eq. (13) to which it reduces for sufficiently small  $g'_p$ . Because of the rather explicit appearance of the interaction potential in this formula, we label the blue lines in Fig. (2) as ‘potential force’. High frequency waves arrive before low-frequency ones, because its larger sound speed. We also see how the frequencies become Doppler-shifted for increasing  $V_p$ . We have derived in Sect. 3.1 several approximate expressions for the inertial force. First, Eq. (21) is obtained with the sole assumption (besides  $g_p$  sufficiently small) of smallness of the unsteady and/or inhomogeneous part  $\delta\psi_0$  of the wavefunction, which allows linearization. Eq. (23) assumes in addition weak inhomogeneities below scales  $a$  and  $\xi$ , and finally Eqs. (25) and (26) (equivalent under the previous linearization approximation) completely neglects such inhomogeneities (or equivalently, they correspond to  $a, \xi \rightarrow 0$ ). We show as black lines in Fig. (2) the prediction of this last approximation, similar to the most standard classical expressions. Since we have computed the wavefunction  $\psi = 1 + \delta\psi_0$  in the comoving frame from Eq. (36), we actually use expression (23) without the Faxén Laplacian terms, with  $\delta\omega^{(0)} = \nabla(\delta\psi_0 - \delta\psi_0^*)/(2i) - \mathbf{V}_p$ , and  $\dot{\mathbf{V}}_p = 0$ . Fig. (36) shows that the full force computed from Eq. (6) is well-captured by the approximate expression of the inertial force for small test-particle size  $a'$ . Accuracy progressively deteriorates for increasing  $a'$ , and also for increasing  $V_p$ , but this classical expression remains a reasonable approximation until  $a' \approx 1$ . The accuracy can be improved by considering higher-order Faxén corrections, Eq. (23), or even better, by considering the integral form in Eq. (21). We have explicitly checked that keeping the full Gaussian integration in Eq. (21) but approximating the integrand in the Bessel integral by its value at the particle position gives a very good

approximation to the exact force even for  $a' = 1$ .

#### 4.2. Numerical evaluation of the drag force

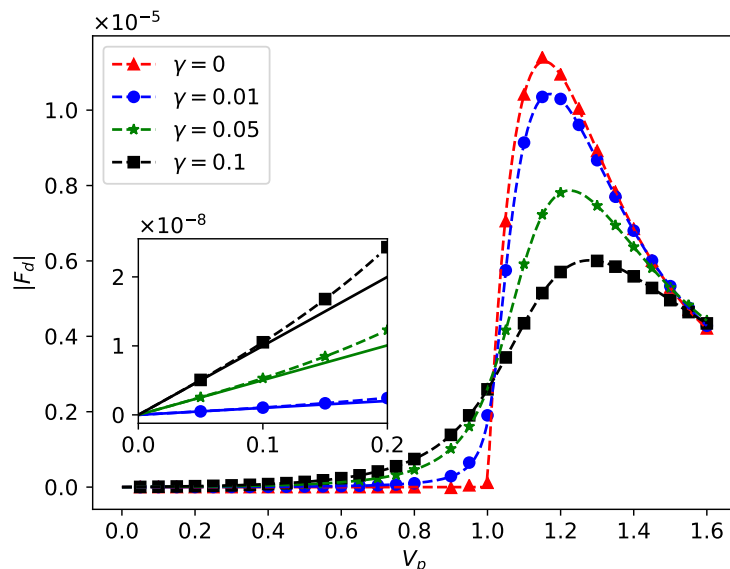


**Figure 3.** Self-induced drag in the steady-state regime as function of the speed  $V_p$ . Dashed lines are the analytical predictions based on Eq. (33) (for  $\gamma = 0$ ) and Eq. (31) (for  $\gamma > 0$ ). The symbols correspond to the numerically computed force from Eq. (6) based on direct simulations of the dGPE Eq. (36). The inset figure shows the small  $V_p$  behavior, with solid straight lines giving the linear dependence of the drag force on the speed for  $\gamma > 0$ , in the small- $V_p$  approximation given by Eq. (35). We use  $a = 1$  and  $g_p = 0.01$ .

We now return to the situation in which there is a single impurity in the system, with size  $a = \xi = 1$  and  $g_p = 0.01$ . It moves in the positive  $x$  direction with speed  $V_p$  producing a perturbation on the uniform and steady condensate state  $\psi = 1$ . We compute it in the comoving frame, in which the particle is at rest and fluid moves with speed  $-V_p$ , by using Eq. (36). Since in the absence of the impurity there is no inhomogeneity nor time dependence,  $\delta\psi_0 = 0$  and the exact force on the impurity, Eq. (6), is also given by the self-induced drag expression given by Eq. (8). After a transient, that in analogy with the results for compressible classical fluids [39, 34] we expect to be of the order of the time needed by the sound waves to cross a region of size  $a$  or  $\xi$ , the condensate density near the particle achieves a steady state, and we then measure the steady drag on the particle. Fig. (3) shows this force, for several values of  $V_p$  and  $\gamma$ , as dots.

The approximate value of the drag force that is obtained under the assumption of small perturbation (small  $g_p$ ) that allows linearisation is shown as dashed lines. It is computed from Eq. (33) for  $\gamma = 0$  and Eq. (31) for  $\gamma > 0$ . The agreement is excellent. As shown in the inset figure, in the regime of small velocities, the self-induced drag is

indeed linearly dependent on the speed with an effective drag coefficient that is well captured by Eq. (35). This Stokes-like drag at small speeds is due to energy dissipation through collisions between the condensate atoms and thermal atoms, quantified by the thermal drag  $\gamma$ . We notice that the dependence of the drag force on  $V_p$  is consistent with having a critical velocity for superfluidity even at  $\gamma > 0$ , in the sense that there is still a relatively abrupt change in the force (sharper for smaller  $\gamma$ ) around a particular impurity speed. The superfluidity of BECs at finite temperature is still an open question. Recent experiments [40, 41] report superfluid below a critical velocity which is related to the onset of fringes [42]. In the dGPE, the steady state drag is always nonzero. Nonetheless, there is a critical velocity associated to the breakdown of superfluidity due to energy dissipation through acoustic excitations. This is the regime where the drag force is dominated by the interaction of the impurity with the supersonic shock waves to produce the Čerenkov wake as seen in Fig. 1(c) and observed experimentally [38]. The maximum drag force occurs near the velocity for which the cusp lines forming the wake still retain an angle close to  $\pi$ . With increasing speed, this angle becomes more acute (Fig. 1(f)), and this lowers the density gradient around the impurity.

## 5. Conclusions

We have studied, from analytic and numerical analysis of the dGPE, the hydrodynamic forces acting on a small moving impurity suspended in a 2D BEC at low temperature. In the regime of small coupling constant  $g_p$  and thermal drag  $\gamma$ , the force arising from the gradient of the condensate density can be decomposed onto the inertial force that is produced by the inhomogeneities and time-dependence of the condensate in the absence of the particle, and the self-induced force which is determined by the perturbation produced by the impurity on the condensate. When the unperturbed flow can be considered homogeneous on scales below the particle size and the condensate coherence length, the classical Maxey and Riley expression [22], giving the inertial force in terms of the local or material fluid acceleration, is a good description of the force. When inhomogeneities become relevant below these scales, Faxén-type corrections arise, similar to the classical ones in the presence of a finite-size particle, but here the coherence length plays a role similar to the particle size. In addition, the condensate thermal drag enters into these expressions, at difference with the classical viscous case. We also determined the self-induced force in the steady-state regime and shown that it is non-zero at any velocity  $V_p$  of the moving impurity if  $\gamma > 0$ . For small  $V_p$ , this force is given as a Stokes drag which is linearly proportional to  $V_p$  with a drag coefficient dependent on the thermal drag  $\gamma$ . The energy dissipation associated with this drag is due to the loss of condensate atoms into the thermal cloud and is mediated by the thermal drag coefficient. In this sense, the drag on the impurity relates to the way the condensate dissipates energy at low temperature through particle exchanges with the thermal cloud. We have not considered the additional drag arising from direct interactions of impurity with the thermal cloud, since these are negligible in the low-temperature regime but maybe important at higher

temperature. With increasing velocities, there are corrections to the linear drag and above a critical speed  $V_c = 1$ , the self-induced drag is dominated by the interactions of the impurity with the emitted shock waves.

We have checked our analytical expressions with numerical simulations in the situation in which the impurity moves at constant velocity, possibly driven by external forces different from the hydrodynamic ones analysed here. When the coupling constant  $g_p$  is sufficiently small so that only the inertial force is relevant, the equation of motion of the impurity under the sole action of the inertial force would be  $m_p d\mathbf{V}_p(t)/dt = \mathbf{F}^{(0)}(t)$ , with  $m_p$  the mass of the particle and  $\mathbf{F}^{(0)}(t)$  one of the suitable approximations to the inertial force given in Sect. 3.1. For larger  $g_p$ , when the condensate becomes distorted by the impurity, we have computed the self-induced drag only in the steady case. In analogy with classical compressible flows [39, 34], we expect history-dependent forces in this unsteady situation. The dependence on the thermal drag, however, would be quite different from that of viscous classical fluids, because of the lack of viscous boundary layers in the BEC case.

In this study, we have focused on a small impurity that can only shed acoustic waves. Another interesting extension of this would be to further investigate the drag and inertial forces for larger impurity sizes, which can emit vortices, and study the effect of vortex-impurity interactions on the hydrodynamics forces. Following the recent experimental progress on testing the superfluidity in BEC at finite temperature [21], it would be interesting to test experimentally our prediction of the linear drag on the impurity due to the condensate thermal drag at small velocities by using measurements of the local heating rate. For probing the inertial force, it would be interesting to experimentally tracking the position of the impurity during non-steady superfluid flow.

## Acknowledgments

We are thankful to Vidar Skogvoll, Kristian Olsen, Zakarias Laberg Hejlesen and Per Arne Rikvold for stimulating discussions. This work was partly supported by the Research Council of Norway through its centers of Excellence funding scheme, Project No. 262644, and by Spanish MINECO/AEI/FEDER through the María de Maeztu Program for Units of Excellence in R&D (MDM- 2017-0711).

## Appendix: Numerical integration of dGPE

Numerical simulations of dGPE Eq. (36) are run for a system size of  $128 \times 256$  (in units of  $\xi$ ) corresponding to the grid size  $dx = 0.25\xi$ , and  $dt = 0.01\xi/c$ . To simulate an infinite domain where the density variations emitted by the impurity do not recirculate under periodic boundary conditions, we use the fringe method from [33]. This means that we define buffer (fringe) regions around the outer rim of the computational domain (see Fig. 4) where the thermal drag  $\gamma$  is much larger than its value inside the domain, such that any density perturbation far from the impurity is quickly damped out and a

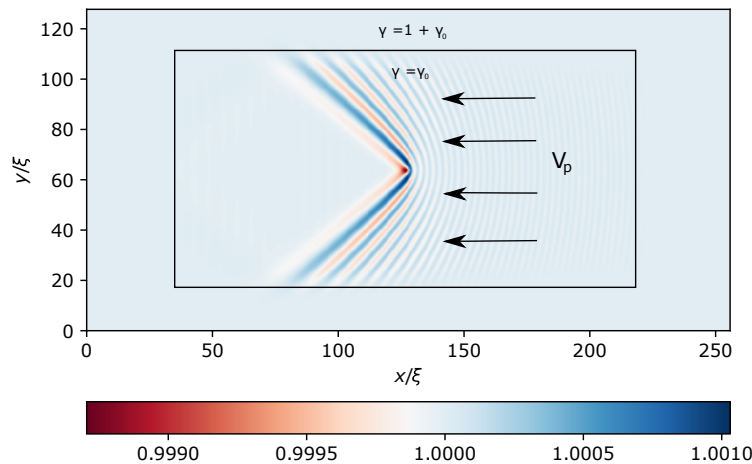


**Figure 4.** Simulation domain showing the buffer region, outside the main simulation region, in which thermal drag is greatly enhanced to eliminate the emitted waves sufficiently far from the moving particle (which is at  $x/\xi = 128$ ,  $y/\xi = 64$ ). The density shown is the steady state (in the comoving frame, hence the direction of the arrows indicating the flow velocity in this frame) for  $V_p = 1.6$  and  $\gamma = 0$ .

steady inflow is maintained. The thermal drag becomes thus spatially-dependent and given by  $\gamma(\mathbf{r}) = \max[\gamma(x), \gamma(y)]$ , where

$$\begin{aligned} \gamma(x) = & \frac{1}{2} (2 + \tanh[(x - x_p - w_x)/d] \\ & - \tanh[(x - x_p + w_x)/d]) + \gamma_0, \end{aligned} \quad (37)$$

and similarly for  $\gamma(y)$ . Here  $\mathbf{r}_p = (x_p, y_p) = (128\xi, 64\xi)$  is the position of the impurity and  $\gamma_0$  is the constant thermal drag inside the buffer regions (bulk region). We set the fringe domain as  $w_x = 100\xi$ ,  $w_y = 50\xi$  and  $d = 7\xi$  as illustrated in Figure 4.

By separating the linear and non-linear terms in Eq. (36), we can write the dGPE formally as [43]

$$\partial_t \psi = \hat{\omega}(-i\nabla)\psi + N(\mathbf{r}, t), \quad (38)$$

where  $\hat{\omega}(-i\nabla) = i[\frac{1}{2}\nabla^2 + 1] + \mathbf{V}_p \cdot \nabla$  is the linear differential operator and  $N(\mathbf{r}, t) = -(i + \gamma)(\mathcal{U}_p + |\psi|^2)\psi + \gamma\psi + \frac{1}{2}\gamma\nabla^2\psi$  is the nonlinear function including the spatially-dependent  $\gamma$  and  $\mathcal{U}_p$ . Taking the Fourier transform, we obtain ordinary differential equations for Fourier coefficients  $\psi(\mathbf{k}, t)$  as

$$\partial_t \hat{\psi}(\mathbf{k}, t) = \hat{\omega}(\mathbf{k})\hat{\psi}(\mathbf{k}, t) + \hat{N}(\mathbf{k}, t), \quad (39)$$

which can be solved by an operator-splitting and exponential-time differentiating method [44]. It means that we exploit the fact that the linear part of Eq. (39) can be solved exactly by multiplying with the integrating factor  $e^{-\hat{\omega}(\mathbf{k})t}$ . This leads to

$$\partial_t \left( \hat{\psi}(\mathbf{k}, t) e^{-\hat{\omega}(\mathbf{k})t} \right) = e^{-\hat{\omega}(\mathbf{k})t} \hat{N}(\mathbf{k}, t). \quad (40)$$

The nonlinear term  $\hat{N}(\mathbf{k}, t)$  is linearly approximated in time for a small time-interval  $(t, t + \Delta t)$ , i.e

$$\hat{N}(\mathbf{k}, t + \tau) = N_0 + \frac{N_1}{\Delta t} \tau \quad (41)$$

where  $N_0 = \hat{N}(t)$  and  $N_1 = \hat{N}(t + \Delta t) - N_0$ . Inserting this into Eq. (40) and integrating from  $t$  to  $t + \Delta t$  we get

$$\begin{aligned} \hat{\psi}(\mathbf{k}, t + \Delta t) &= \hat{\psi}(\mathbf{k}, t) e^{\hat{\omega}(\mathbf{k})\Delta t} + \frac{N_0}{\hat{\omega}(\mathbf{k})} (e^{\hat{\omega}(\mathbf{k})\Delta t} - 1) \\ &+ \frac{N_1}{\hat{\omega}(\mathbf{k})} \left[ \frac{1}{\hat{\omega}(\mathbf{k})\Delta t} (e^{\hat{\omega}(\mathbf{k})\Delta t} - 1) - 1 \right]. \end{aligned} \quad (42)$$

Since computing the value of  $N_1$  requires knowledge of the state at  $t + \Delta t$  before we have computed it, we start by setting it to zero and find a value for the state at  $t + \Delta t$  given that  $\hat{N}(t)$  is constant in the interval. We then use this state to calculate  $N_1$ , and add corrections to the value we got when assuming  $N_1 = 0$ .

## References

- [1] Winiecki T and Adams C S 2000 *EPL (Europhysics Letters)* **52** 257
- [2] Wouters M and Carusotto I 2010 *Physical Review Letters* **105** 020602
- [3] Astrakharchik G E and Pitaevskii L P 2004 *Physical Review A* **70** 013608
- [4] Shukla V, Brachet M and Pandit R 2016 *Physical Review A* **94** 041602
- [5] Pinsker F 2017 *Physica B: Condensed Matter* **521** 36–42
- [6] Poole D R, Barenghi C F, Sergeev Y A and Vinen W F 2005 *Physical Review B* **71** 064514
- [7] Chikkatur A P, Görlitz A, Stamper-Kurn D M, Inouye S, Gupta S and Ketterle W 2000 *Physical Review Letters* **85** 483
- [8] Zipkes C, Palzer S, Sias C and Köhl M 2010 *Nature* **464** 388
- [9] Balewski J B, Krupp A T, Gaj A, Peter D, Büchler H P, Löw R, Hofferberth S and Pfau T 2013 *Nature* **502** 664
- [10] Jørgensen N B, Wacker L, Skalmstang K T, Parish M M, Levinsen J, Christensen R S, Bruun G M and Arlt J J 2016 *Physical Review Letters* **117** 055302
- [11] Pham C T, Nore C and Brachet M E 2005 *Physica D: Nonlinear Phenomena* **210** 203 – 226" ISSN 0167-2789 URL <http://www.sciencedirect.com/science/article/pii/S0167278905003167>
- [12] Berloff N G and Roberts P H 2000 *Phys. Rev. B* **63**(2) 024510 URL <https://link.aps.org/doi/10.1103/PhysRevB.63.024510>
- [13] Griffin A, Stagg G W, Proukakis N P and Barenghi C F 2017 *Journal of Physics B: Atomic, Molecular and Optical Physics* **50** 115003
- [14] Shukla V, Pandit R and Brachet M 2018 *Phys. Rev. A* **97**(1) 013627 URL <https://link.aps.org/doi/10.1103/PhysRevA.97.013627>
- [15] Giuriato U and Krstulovic G 2019 *Scientific Reports* **9** 4839
- [16] Roberts D C 2006 *Physical Review A* **74** 013613
- [17] Roberts D C and Pomeau Y 2005 *Physical Review Letters* **95** 145303
- [18] Pomeau Y and Roberts D C 2008 *Physical Review B* **77** 144508
- [19] Sykes A G, Davis M J and Roberts D C 2009 *Physical Review Letters* **103** 085302
- [20] Pinsker F 2017 *New Journal of Physics* **19** 113046
- [21] Singh V P, Weimer W, Morgener K, Siegl J, Hueck K, Luick N, Moritz H and Mathey L 2016 *Physical Review A* **93** 023634
- [22] Maxey M R and Riley J J 1983 *The Physics of Fluids* **26** 883–889

- [23] Gardiner C W, Anglin J R and Fudge T I A 2002 *Journal of Physics B: Atomic, Molecular and Optical Physics* **35** 1555
- [24] Rooney S J, Blakie P B and Bradley A S 2012 *Physical Review A* **86** 053634
- [25] Penckwitt A A, Ballagh R J and Gardiner C W 2002 *Physical Review Letters* **89** 260402
- [26] Bradley A S and Anderson B P 2012 *Physical Review X* **2** 041001
- [27] Reeves M T, Billam T P, Anderson B P and Bradley A S 2013 *Physical Review Letters* **110** 104501
- [28] Reeves M T, Billam T P, Anderson B P and Bradley A S 2014 *Physical Review A* **89** 053631
- [29] Skaugen A and Angheluta L 2016 *Physical Review E* **93** 032106
- [30] Bradley A S, Gardiner C W and Davis M J 2008 *Physical Review A* **77** 033616
- [31] Billam T P, Reeves M T and Bradley A S 2015 *Physical Review A* **91** 023615
- [32] Neely T W, Bradley A S, Samson E C, Rooney S J, Wright E M, Law K J H, Carretero-González R, Kevrekidis P G, Davis M J and Anderson B P 2013 *Physical Review Letters* **111** 235301
- [33] Reeves M T, Billam T P, Anderson B P and Bradley A S 2015 *Physical Review Letters* **114** 155302
- [34] Parmar M, Haselbacher A and Balachandar S 2012 *Journal of Fluid Mechanics* **699** 352–375
- [35] Pismen L M 1999 *Vortices in nonlinear fields: From liquid crystals to superfluids, from non-equilibrium patterns to cosmic strings* vol 100 (Oxford University Press)
- [36] Dalfovo F, Giorgini S, Pitaevskii L P and Stringari S 1999 *Rev. Mod. Phys.* **71**(3) 463–512 URL <https://link.aps.org/doi/10.1103/RevModPhys.71.463>
- [37] See supplementary material at <https://cloud.ifisc.uib-csic.es/nextcloud/index.php/s/AFzw6JxNW77DT6d> showing movies of the condensate density dynamics at  $\gamma = 0$  and several values of  $V_p$ .
- [38] Carusotto I, Hu S X, Collins L A and Smerzi A 2006 *Physical Review Letters* **97** 260403
- [39] Longhorn A L 1952 *The Quarterly Journal of Mechanics and Applied Mathematics* **5** 64–81 ISSN 0033-5614
- [40] Singh V P, Weimer W, Morgener K, Siegl J, Hueck K, Luick N, Moritz H and Mathey L 2016 *Phys. Rev. A* **93**(2) 023634 URL <https://link.aps.org/doi/10.1103/PhysRevA.93.023634>
- [41] Weimer W, Morgener K, Singh V P, Siegl J, Hueck K, Luick N, Mathey L and Moritz H 2015 *Physical Review Letters* **114**(9) 095301 URL <https://link.aps.org/doi/10.1103/PhysRevLett.114.095301>
- [42] Wouters M and Carusotto I 2010 *Physical Review Letters* **105**(2) 020602 URL <https://link.aps.org/doi/10.1103/PhysRevLett.105.020602>
- [43] Skaugen A 2018 *A unified perspective on two-dimensional quantum turbulence and plasticity* Ph.D. thesis University of Oslo
- [44] Cox S M and Matthews P C 2002 *Journal of Computational Physics* **176** 430–455